Journal of Theoretical and Applied Information Technology
15th February 2023. Vol.101. No 3

ISSN: 1992-8645 www.jatit.org E-ISSN: 1817-3195

A NOVEL APPROACH FOR QR CODE IMAGE BASED ON DECIMAL CODING TECHNIQUE, GRAY LEVEL CO-OCCURRENCE MATRIX AND LOCAL BINARY PATTERN

TOUFIK DATSI[1*], KHALID AZNAG[1], AHMED EL OIRRAK[1]

[1]Department of Computer Science, Cadi Ayyad University, Marrakech, Morocco

E-mail: [1*]toufik.datsi@ced.uca.ma, [1]khalid.aznag@ced.uca.ac.ma, [1]oirrak@uca.ac.ma

ABSTRACT

Image description is an important task in image processing. Current image description techniques are based on grayscale and color image. In this paper, we propose an efficient approach for a QR code image description that combines a decimal coding technique with a gray-level co-occurrence matrix (GLCM) and a local binary pattern (LBP). This approach involves extracting the characteristics of the initial image by transforming the binary representation into a decimal value, i.e., by encoding each row of the image as a decimal value. All the values calculated from the image are regrouped into a matrix, which is used to extract a gray-level co-occurrence matrix and local binary pattern. The proposed method has been implemented using QR code dataset. Experiments show that the proposed approach effectively describes the QR code images and gives the best results in terms of GLCM properties, the histogram of the LBP, and the execution time.

Keywords: *Texture Analysis, Image Description, Decimal Coding, Gray-Level Co-occurrence Matrix, Local Binary Pattern*

1. INTRODUCTION

The texture of an image is considered an important feature in the field of image processing and is widely used in a variety of applications, such as facial recognition [1], document image analysis [2], biomedical applications, and remote sensing [3]. The purpose of texture analysis is to extract the characteristics of the image and to express them in the form of a feature vector. Texture analysis methods are used to quantify the different textures present in an image [4]. These analysis techniques have better discriminative power than the eye-brain set, which is less able to process complex texture variations. Several methods of texture analysis exist, and they can be classified into two main categories: structural methods and statistical methods. In structural methods, the texture analysis is based on the description of the primitives and on the formalization of the spatial relationship between these primitives. The statistical methods study the relationship between a pixel and its neighborhood. They are generally used to characterize fine structures with no apparent regularity. Based on the number of pixels, the statistical methods can be divided into first-order statistics, second-order statistics, and higher-order statistics [5]. The first-order statistical methods are based on first-order histograms [6]. Such histograms indicate the frequency of appearance of a gray level in a considered neighborhood. Several statistical parameters of different degrees can be extracted from these histograms. Among the statistics frequently used to describe a texture are the mean, variance, and entropy [7]. The limitation of first-order statistics is that the parameters calculated take into account only the histogram of the image. However, two different images with different textures can have the same histogram. It is thus essential to integrate information concerning the locations of pixels: one should not utilize only the number of gray levels in the image. To do this, one must move on to a texture analysis method using second- and higher-order statistics. These methods include the gray-level co-occurrence matrix (GLCM), [8] local binary pattern (LBP) [9], auto-correlation function [10], etc. The GLCM and LBP methods are feature extraction techniques commonly used for texture analysis, especially in the automatic recognition of code.

The recognition of quick response (QR) codes is considered one of the most challenging research areas in the field of computer vision [11]. Created by the Japanese company Denso Wave in 1994, a QR code is a type of two-dimensional barcode (or

matrix code) consisting of black modules arranged in a square with a white background. Each module represents either 1 or 0. The arrangement of these modules defines the information contained in the QR code. Intended to automate the acquisition of generally digital information, the QR code has been applied in a variety of fields, including medicine [12], education [13], industry [14], etc. An example of a QR code is shown in Figure 1.

The task of characterizing the texture of large QR codes poses a significant challenge such as size and nature of image [8, 9], and calls for innovative techniques. Current methods for extracting features from images, such as Local Binary Patterns (LBP) and Gray-level Co-occurrence Matrix (GLCM), primarily rely on gray-scale images. This research proposes a new method for feature descriptor of binary images. The method involves utilizing decimal coding technique to calculate the GLCM and LBP of the binary image, and subsequently utilizing the properties of both GLCM and LBP to describe the texture.

The remainder of the paper is organized as follows. An overview of some previous work in the literature is presented in section 2. The Methodology, which includes the proposed scheme, is explained in section 3. Section 4 provides a discussion of the results obtained, and section 5 concludes the paper.

Figure 1: An Example of QR Code Image

2. RELATED WORK

Several approaches have been proposed in the literature to describe and detect QR code images. [15] proposed a scheme based on a local binary pattern and a contour image for QR code detection. The scheme is divided into three phases: image preprocessing, QR code rough detection, and QR code precise detection. The image processing phase consists of converting the input image into a gray image; then, the median filter is used for image noising and the adaptive Bernsen method is applied for image binarization. In the QR code rough detection, the local binary pattern is combined with contour approximation for detection results. For the QR code precise detection phase, the Finder Pattern special pixel ratio is used. Experiments show that the system has a recall rate of 83% and a precision rate of 93%. [16] presented a novel approach for the fast detection of QR codes based on run-length coding. The connected component values are connected to locate the minimum region containing the position detection pattern (PDP) in the QR code; then, the run-length coding is applied to calculate the central coordinate of the PDP in the QR code. The results show that the proposed approach is efficient in terms of the running time of locating QR codes. [17] Evaluated different deep learning techniques and adopted an architecture based on a single-shot object detector algorithm. This architecture facilitates detection through the annotation of object subparts. The proposed technique was applied to both QR codes and Finder Patterns. [18] Proposed an algorithm for precisely locating 2D QR codes in arbitrary images with varying illumination conditions. This algorithm performs image binarization and then QR code localization using the characteristics of Finder Patterns and finally identifies perspective distortion. The proposed method was tested using 595 QR code samples and was shown to have a high detection rate. [19] Presented a framework for recognizing QR codes in complex background images. The proposed method uses the convolutional neural network (CNN) architecture and a spatial pyramid to detect partial barcode patches. The system was evaluated with 125 QR codes and achieved an accuracy rate of 95.2%. [20] Developed an approach that optimizes QR code detection from different angles. The preprocessing of the images, a CNN architecture, and QR code detection are the principal blocks of the proposed system. Experiments show that the proposed method has an accuracy rate of 90%. The results demonstrated that the system has a high potential to detect QR codes from the wider Euler angle. [21] proposed a new method for the binarization and recognition of QR codes. The Otsu method is combined with the Bernsen method and the various thresholds are selected for the binarization of the image. The proposed technique was evaluated with 100 images of 680×480 pixels. The results show that the proposed method achieves an accuracy of 96% on the recognition of QR code images.

3. METHODOLOGY

In this work, two texture features extractors, namely the GLCM and LBP methods have been implemented separately and combined with the

proposed technique to describe black and white images.

3.1 Gray Level Co-occurrence Matrix

Introduced by Haralick [22], the gray-level co-occurrence matrix (GLCM) is considered an effective method that is widely used for image texture analysis. It represents the relative- position spatial information between different pixel pairs; in other words, the GLCM reflects the spatial distribution of various gray levels in the texture image [23]. The calculation of a gray-level co-occurrence matrix consists of locating in an image the number of occurrences of pairs of gray levels separated by a distance d in a direction defined by a displacement vector dx, dy [22]. The calculation of the GLCM for an image I with dimensions $N \times N$ is formalized as follows:

$$P(k,j)=\sum_{n=1}^{N}\sum_{m=1}^{N}\begin{cases}1, \text{ if } (m,n)=k \text{ and } I(n+dx, m+dy)=j\\ 0, \text{ otherwise}\end{cases} \quad (1)$$

Where N is the number of gray levels; k and j are the gray levels of the reference pixel and the neighboring pixel, respectively; n and m correspond to the coordinates of the pixels in image I. The distance between the pixel of interest and its neighbor is specified by the offset (dx, dy). From (1), we notice that the inputs near the diagonal of the matrix of co-occurrence will be higher the closer the grayscale values of the image are the travel distance in question. On the other hand, non-diagonal inputs will be higher for images in which the gray levels vary locally for the displacement under consideration. Similarly, the textural content will be expressed differently depending on the distance and orientation of the movement considered between pairs of sites. The GLCM is calculated for four different orientations $(0^0, 45^0, 90^0, 135^0)$ for the same travel distance according to the recommendation by Haralick [22]. Figure 2 represents the spatial relationships between the pixel of interest and other pixels.

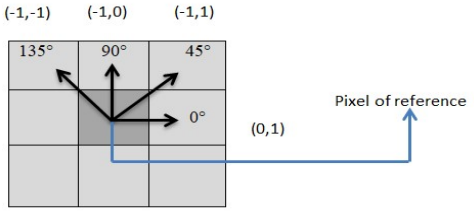

Figure 2: Spatial Relationships Between the Pixel of Interest and Other Pixels

The element of the gray co-matrix is equal to the number of pairs of pixels in the image, such that the one brightness is k and its 'neighbor at a distance of d and an angle θ brightness j. The GLCM dimension is determined by the number of gray levels in the image, for example, for an image with a color depth of 8 bits the matrix will have 256 rows and 256 columns. Figure 3 illustrates an example of a GLCM calculation with $N_g = 5$ levels.

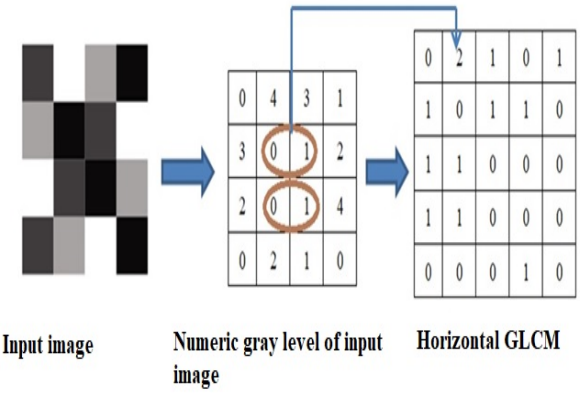

Figure 3: GLCM Calculation with Level =5

Fourteen original statistics features are proposed by Haralick to measure the feature texture using the co-occurrence matrix [23]. Out of Haralick's 14 features, the proposed method extracts the contrast, energy, homogeneity, and entropy, as they are the most frequently used features [24]. These four features are extracted from the GLCM; they are summarized as follows.

- The contrast measures the gray level variation in GLCM matrix. It indicates the relation between the pixel and its neighbor by computing the intensity.

$$contrast\ (d,\theta) = \sum_{i=0}^{N_g-1}\sum_{j=0}^{N_g-1}(i-j)^2\ P_d{}^{\theta}(i,j) \quad (2)$$

- The uniformity of the not zero in the GLCM is computed by Homogeneity. The Homogeneity value ranges from 0 to 1.

$$Hom\ (d,\theta) = \sum_{i=0}^{N_g-1}\sum_{j=0}^{N_g-1}\frac{1}{1+(i-j)^2}\ P_d{}^{\theta}(i,j) \quad (3)$$

- The energy expresses the regular character of the texture. It measures the disorder of an image. The Energy is expected to be high if the occurrence of repeated pixel pairs is high, given by:

$$Energy\ (d,\theta)= \sum_{i=0}^{N_g-1}\sum_{j=0}^{N_g-1}\left[P_d^{\ \theta}(i,j)\right]^2 \quad (4)$$

- The correlation indicates the degree of linear linkage that exists between the different occurrences of the image.

$$corre(d,\theta)= \sum_{i=0}^{N_g-1}\sum_{j=0}^{N_g-1}\frac{ij\ P_d^{\ \theta}(i,j)-\mu_x\mu_y}{\sigma_x\sigma_y} \quad (5)$$

where μ_x and μ_y designate the GLCM means based on the reference pixel $P(x,y)$ and its neighbor pixel respectively. μ_x and μ_y are given as

$$\mu_x = \sum_{i=0}^{N_g-1}\sum_{j=0}^{N_g-1} i.P_{d,\theta}(i,j) \quad (6)$$

$$\mu_y = \sum_{i=0}^{N_g-1}\sum_{j=0}^{N_g-1} j.P_{d,\theta}(i,j) \quad (7)$$

σ_x and σ_y represent the standard deviations based on the reference pixel and its neighbor pixel, respectively; they are expressed as

$$\sigma_x = \sqrt{\sum_{i=0}^{N_g-1}\sum_{j=0}^{N_g-1}(i-\mu_x)^2 P_{d,\theta}(i,j)} \quad (8)$$

$$\sigma_y = \sqrt{\sum_{i=0}^{N_g-1}\sum_{j=0}^{N_g-1}(j-\mu_y)^2 P_{d,\theta}(i,j)} \quad (9)$$

3.2 Local Binary Pattern

The local binary pattern (LBP) is an operator that describes a pixel's environment by generating a bit code from the pixels binary derivatives [25, 26]. The operator is typically applied to images in gray scale and images with derived intensities. As illustrated in Figure 4, the LBP operator was defined on a 3×3 pixel block consisting of a center pixel with 8 neighbors; the center pixel value was taken as the threshold value. If the surrounding neighborhood pixel's value is greater than or equal to the threshold value, the neighborhood pixel's position is given a value of 1; otherwise, the neighborhood pixel's position is given a value of 0. All of the obtained binary values are multiplied by the weights of the corresponding pixels positions and summed to calculate the LBP value.

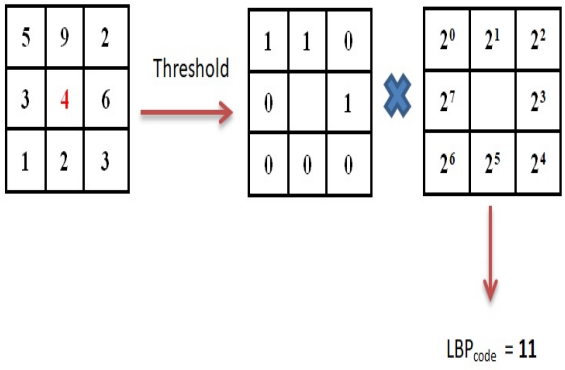

Figure 4: An Example of the Calculation of the LBP Operator

The LBP operator is defined by the following equation:

$$LBP_{P,R}(x_c,y_c) = \sum_{p=0}^{p-1} s(i_p - i_c)2^p \quad (10)$$

Where R is the neighborhood radius, i_c is the gray scale value of the center pixel, P represents the number of the neighborhood pixels around the center pixel (x_c,y_c), i_p denotes the first neighborhood grayscale values of a pixel point. The function $S(t)$ is defined as

$$s(t) = \begin{cases} 1, & t \geq 0 \\ 0, & t \prec 0 \end{cases} \quad (11)$$

3.3 Proposed Model

In this work, the proposed scheme comprised three major phases: the decimal coding phase, feature extraction phase, and result phase. The model phases can be summarized in Figure 5.

Journal of Theoretical and Applied Information Technology
15th February 2023. Vol.101. No 3

ISSN: 1992-8645 www.jatit.org E-ISSN: 1817-3195

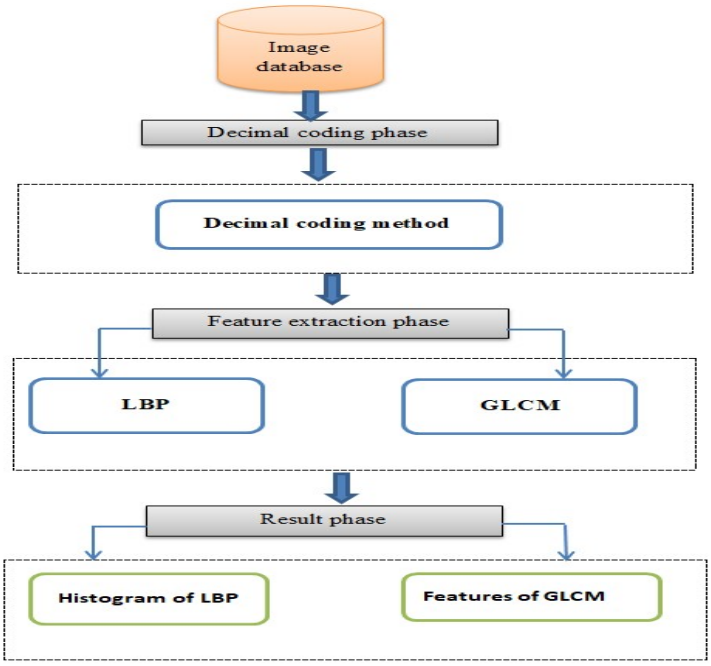

Figure 5: The Proposed Scheme

3.3.1 Decimal Coding Phase

The objective of this method is to calculate the gray-level co-occurrence matrix and local binary pattern for a binary image, where each pixel in the image is stored as a single bit –i.e., a 0 or 1. The technique is divided into three steps. The first step consists of reading the input image and dividing it into a set of blocks of 4×4 pixels. In the second step, for each block we encode each row using a decimal value; then, we get a matrix that represents all the values encoded by decimal coding with levels of gray. This method help us to convert the binary image to grayscal image and then use this last image to found the gray co-matrix and local binary for binary image. The process of decimal coding is illustrated in Figure 7.

3.3.2 Feature Extraction Phase

After dividing the initial image into blocks and encoding each row of the blocks using a decimal value, for feature extraction based on the GLCM and LBP, we calculate for each block of the binary image the co-occurrence matrix and the local binary pattern.

3.3.3 Result Phase

In this last phase, the histogram of the LBP of each image and the features of the GLCM are calculated and displayed. For the GLCM we calculate the contrast, homogeneity, energy, and correlation. Figure 6 illustrate the block diagram of GLCM and histogram of LBP obtained in result phase.

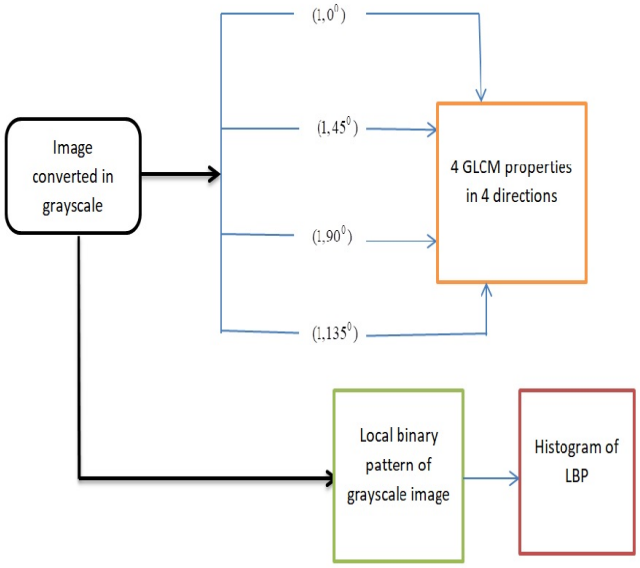

Figure 6: The Block Diagram of GLCM and LBP in Result Phase

ISSN: 1992-8645 www.jatit.org E-ISSN: 1817-3195

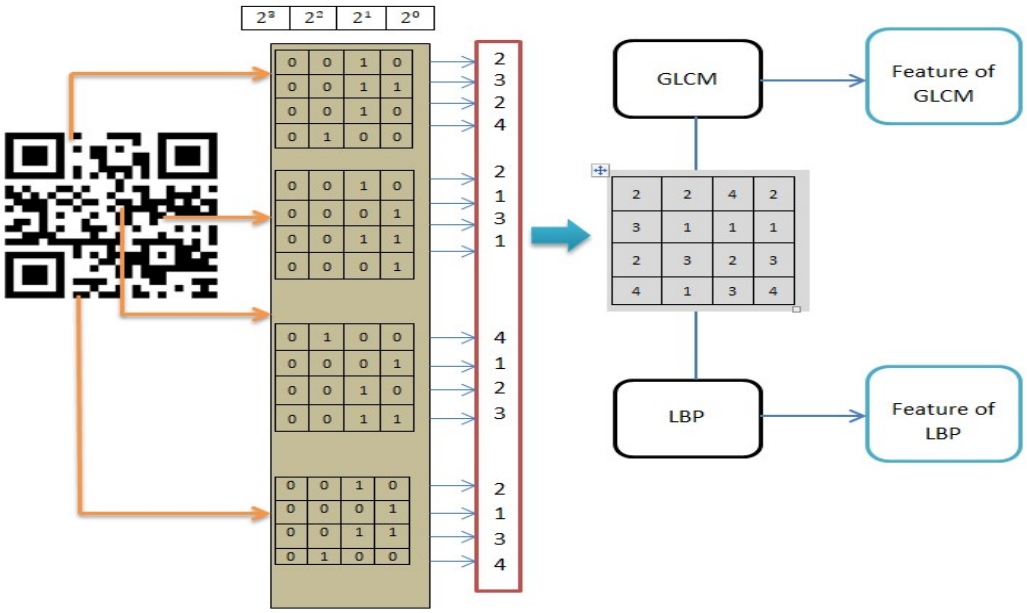

Figure 7: The Process of Decimal Coding

4. RESULTS AND DISCUSSION

The present section discusses the results obtained after applying the proposed method. The experiments were carried out on the Anaconda platform with Python in a Windows 10 environment on an Intel i7 2.2 GHz processor with 12 GB of RAM. The NumPy, skimage, Matplotlib, and scikit-learn libraries were used to implement the methods proposed in this work.

In order to evaluate our approach, the simulation was conducted on binary images. The proposed technique was tested using a QR code database uploaded from Kaggle platform [27]. This database contains 10,000 images, and the size of the images varied from 290×290 pixels to 410×410 pixels. Each QR code image in the dataset has a four version of the QR code encoded by a random four-digit number. For example 1002 represent a QR code with four number digits and with four versions.

4.1 Image Testing with Decimal Coding and GLCM

For the purpose of testing the effectiveness of our method using the GLCM, we have tested the decimal coding technique with different images selected in the dataset. Figure 8 shows the results of the converting binary images of QR code into grayscale image by applying the decimal coding method for different images of QR codes.

To analyze GLCM properties, four texture features were calculated for various angles for all patterns selected. Tables 1-4 display the values of four texture features, i.e., the contrast, homogeneity, energy, and entropy, calculated for different pairs of angles for 10 different images. From Table 1, it can be seen that the largest value of the contrast in direction 0 was 0.9568. In the same direction, the homogeneity was 0.8631, the energy was 0.7133, and the correlation was 0.9289. Table 2 shows that the largest value of the contrast in direction 45 was 0.9654. In the same direction, the homogeneity was 0.8983, the energy was 0.7562, and the correlation was 0.9222. Table 3 shows that the largest value of the contrast in direction 90 was 0.4922. In the same direction, the homogeneity was 0.9211, the energy was 0.7567, and the correlation was 0.9931. Table 4 shows that the largest values of the contrast, homogeneity, energy in direction 135 were 0.7021, 0.8734, and 0.7068, respectively.

 Image 1	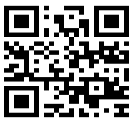 Image 2	 Image 3	 Image 4	 Image 5
 Grayscale image 1	 Grayscale image 2	 Grayscale image 3	 Grayscale image 4	 Grayscale image 5

Figure 8 :The Conversion of the Binary Images into Grayscal Images

Table 1: Four Textures Features for the Angle 0^0 .

Images	Contrast	Homogeneity	Energy	Correlation
Image 1	0.2675	0.7484	0.6174	0.8927
Image 2	0.2974	0.7036	0.5154	0.9055
Image 3	0.2430	0.5666	0.4197	0.8614
Image 4	0.572	0.5489	0.4821	0.8346
Image 5	0.7945	0.3642	0.4381	0.7335
Image 6	0.9568	0.4764	0.3742	0.6678
Image 7	0.3218	0.6628	0.6073	0.8453
Image 8	0.9401	0.8188	0.6956	0.9289
Image 9	0.1998	0.8631	0.6246	0.8209
Image 10	0.2026	0.7570	0.7133	0.1758

Table 2: Four Textures Features for the Angle 45^0 .

Images	Contrast	Homogeneity	Energy	Correlation
Image 1	0.2579	0.8317	0.6603	0.8968
Image 2	0.3052	0.7873	0.5613	0.9031
Image 3	0.2128	0.6069	0.4342	0.8789
Image 4	0.5127	0.6487	0.5122	0.8324
Image 5	0.8016	0.5002	0.4536	0.7302
Image 6	0.9654	0.6040	0.4355	0.6653
Image 7	0.3223	0.7753	0.6690	0.8455
Image 8	0.1065	0.8762	0.7303	0.9222
Image 9	0.2041	0.8983	0.6483	0.8176
Image 10	0.2053	0.511	0.7562	0.1667

Table 3: Four Textures Features for the Angle 90^0 .

Images	Contrast	Homogeneity	Energy	Correlation
Image 1	0.3230	0.8527	0.6721	0.9868
Image 2	0.2837	0.8390	0.5936	0.9909
Image 3	0.2226	06474	0.4587	0.9867
Image 4	0.3498	0.7285	0.5424	0.9887
Image 5	0.4922	0.6068	0.4805	0.9839
Image 6	0.3613	0.6223	0.4690	0.9873
Image 7	0.1399	0.8294	0.7049	0.9931
Image 8	0.1882	0.9067	0.7502	0.9859
Image 9	0.1813	0.9211	0.6652	0.9834
Image 10	0.2166	0.8494	0.7567	0.9100

Table 4: Four Textures Features for the Angle 135^0 .

Images	Contrast	Homogeneity	Energy	Correlation
Image 1	0.5604	0.7448	0.6147	0.7789
Image 2	0.6456	0.7037	0.5155	0.7960
Image 3	0.5342	0.5766	0.4296	0.7019
Image 4	0.1110	0.5381	0.4920	0.6307
Image 5	0.1675	0.3740	0.4410	0.4183
Image 6	0.7021	0.6527	0.6071	0.6705
Image 7	0.2090	0.8287	0.7068	0.8500
Image 8	0.3850	0.8734	0.6346	0.6572
Image 9	0.2676	0.7671	0.7123	0.7126
Image 10	0.5604	0.7448	0.6147	0.7789

4.2 Image Testing With Decimal Coding and LBP

To assess the effect of the proposed technique using the LBP, we have tested this technique using the same dataset with different images. Figure 9 shows the local binary patterns of different grayscale QR code images. After obtaining the grayscale image with decimal coding in our experiments, we calculated the histogram of each QR code image tested. Figures 10-14 shows the histogram of the LBP of grayscale images 1, 2, 3, 4, and 5, respectively. These selected images have different sizes. We can observe that high gray-level intensity is visible in Figures 11-13, when low gray-level intensity is given in Figure 10 and Figure 14.

ISSN: 1992-8645 www.jatit.org E-ISSN: 1817-3195

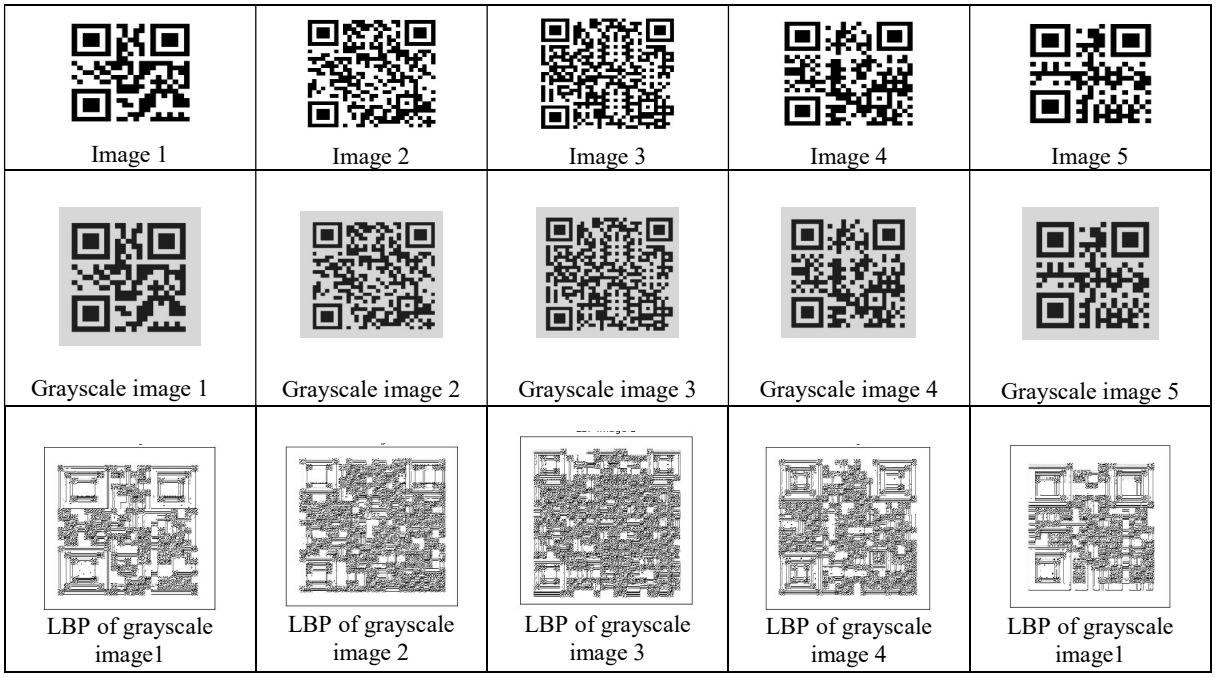

Figure 9: The Local Binary Pattern of Different Grayscale QR Code Images

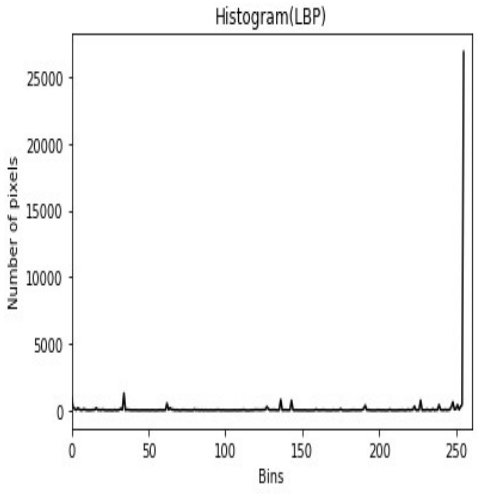

Figure 10: Histogram of LBP of Grayscale Image 1

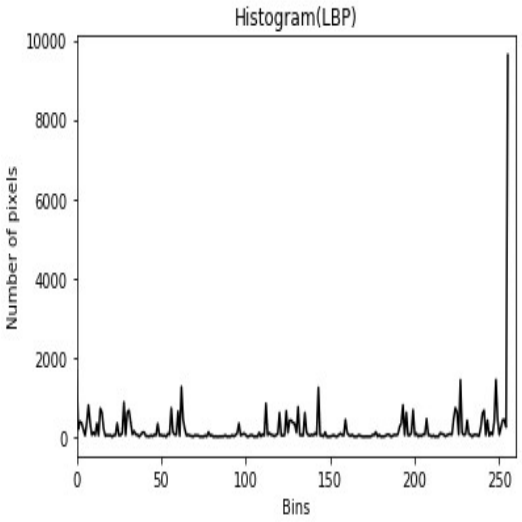

Figure 11: Histogram of LBP of Grayscale Image 2

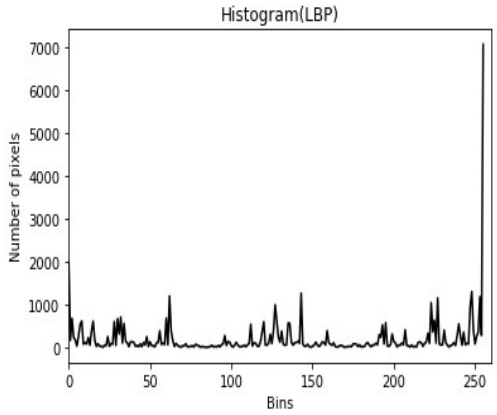

Figure 12: Histogram of LBP of Grayscale Image 3

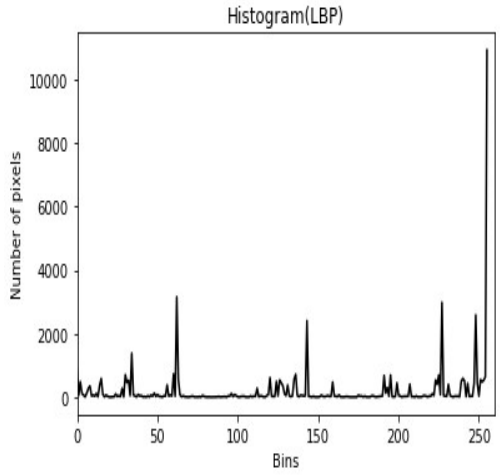

Figure 13: Histogram of LBP of Grayscale Image 4

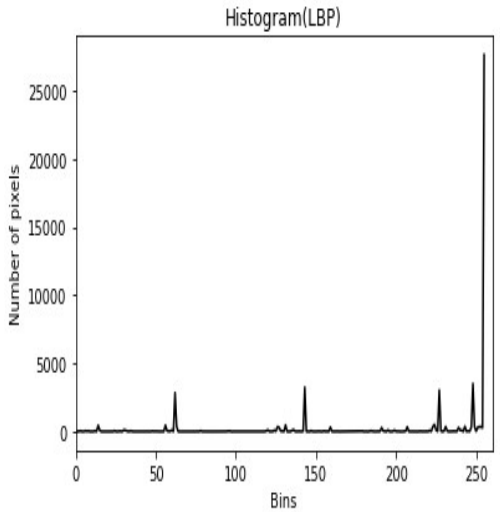

Figure 14: Histogram of LBP of Grayscale Image 5

4.3 Comparison

Table 5 shows the results of comparison of execution time between the decimal coding method using GLCM and the decimal coding method using LBP for different image sizes. Comparing the results below, it can be seen that the decimal coding method applied using GLCM gives the best execution time for different image sizes than if we applied the same method using LBP.

Table 5: Execution Time Performance of Decimal Coding using Both GLCM and LBP

Method	Image size	Execution time (s)
Decimal coding + GLCM	290×290	0.35
	330×330	0.41
	370×370	0.46
	410×410	0.51
Decimal coding + LBP	290×290	0.39
	330×330	0.43
	370×370	0.49
	410×410	0.54

The advantage of our method is that can describe a binary image by converting into grayscale without losing the relevant information, and then found the GLCM and LBP of this binary image. Instead, we can develop our method to take in consideration the problem of rotation and noise for another work.

5. CONCLUSION

In this work, we have proposed an approach for describing QR code images. Our approach is based on using decimal coding to convert binary images into grayscale images, and then calculating the Gray Level Co-occurrence Matrix (GLCM) and Local Binary Patterns (LBP) features of the input image. The image is divided into a set of blocks of pixels, and each row of the image is encoded by a decimal value using the decimal coding method. After extracting the results, we calculated the GLCM features and the histogram of the LBP for each image. The method was tested using a QR code database from the Kaggle platform. The results obtained indicate that the proposed model performs well in terms of the GLCM features and gray-level intensity. Furthermore, the decimal coding with GLCM outperforms more than the same technique with LBP in term of execution time.

Improving the system so that it can classify QR code images with noise and rotated QR code images research.

REFERENCES:

[1] E. G. Moung, J. A. Dargham, A. Chekima and S. Omatu, "Face Recognition State-of-the-art, Enablers, Challenges and Solutions: A Review," *International Journal of Advanced Trends in Computer Science and Engineering*, vol.9, pp. 96–105, 2020.

[2] U. D. Dixit and M. S. Shirdhonker, "A survey on document image analysis and retrieval system," *International Journal on Cybernetics & Informatics*, vol. 9, no. 4, pp. 259–270, 2015.

[3] R. Jiang, "Hyperspectral Remote Sensing Image Classification Based on Deep Learning," *Proceedings of 2020 International Conference on Mechanical Automation and Computer Engineering*, ShaanXi, Chiina, 2020, pp. 042185.

[4] M. Ganga, N. Janakirman, A. K. Sivaraman, A. Balasundaram, R. Vincent, and M. Rajesh," Survey of Texture Based Image Processing and Analysis with Differential Fractional Calculus Methods," *Proceedings of 2021 International Conference on System, Computation, Automation and Networking*, Puduchery, India, 2021, pp.1–6,

[5] A. Ramola, A. K. Shakya, and D. V. Pham, "Study of statistical methods for texture analysis and their modern evolutions," *Engineering Reports, vol. 2, no. 4, 2020.*

[6] A. Bashir, M. Garelnabi, S. Khojlay, M. Hassan and S. Elfadil, "Comparison between the First Order Statistical Analysis and Higher Order Statistical Analysis on Characterization of Brain Tumor on CT Images*," International Journal of Science and Research, vol. 7, no. 8, pp.459–466, 2017.*

[7] L. Malliga, "A Novel Statistical Based Methodology for the Feature Extraction of both MRI and CT images," *International Journal of Engineering and Advanced Technology," vol. 8, no. 6S3, 2019.*

[8] Y. Tao and Y. He, "Face Recognition Based on LBP Algorithm" *Proceedings of 2020 International Conference on Computer Network, Electronic and Automation (ICCNEA), Xian, China, 2020, pp. 21–25.*

[9] C. Liu, A. Xu, C. Hu, F. Zhang , F. Yan, and S. Cai "A New Texture Feature Based on GLCM and Its Application on Edge-detection," *Proceedings IOP Conference Series: Materials Science and Engineering, 2020.*

[10] X. Ding, "Texture Feature Extraction Research Based on GLCM-CLBP Algorithm," *Proceedings of 7th International Conference on Education, Management, Information and Mechanical Engineering (EMIM 2017),2017, pp. 167–171.*

[11] Q. Yan, X. Ji, and Y. Liang, "Displacement detection method of QR code reference object based on computer vision," *Proceedings of 2020 IEEE International Conference on Parallel & Distributed Processing with Applications, Big Data & Cloud Computing, Sustainable Computing & Communications, Social Computing & Networking (ISPA/BDCloud/SocialCom/SustainCom), Exeter, United Kingdom,2020, pp. 895–900.*

[12] A. Boonyapalanant, M. Kectcham, and M. Piyaneeranart, "Hiding patient injury information in medical images with QR code," *Proceedings International Conference on Computing and Information Technology, pp. 258–267, 2019.*

[13] F. Alfiah and A. Youndari, "Design of web-based QR-code absence at the education office," *IAIC Transaction on Sustainable Digital Innovation, vol. 1, no. 1, pp. 26–31, 2019.*

[14] V.V. Patil, M. P. P. Patil, and M. A. B. Toradmal, "Application of Quick Response [QR] code for Digitalization of Plant Taxonomy," *Journal of Information and Computational Science," vol. 10, no.1, pp. 1287-1293, 2020.*

[15] L. Tong, X. Gu, and F. Dai, "QR code detection based on local features," *Proceedings of International Conference on Internet Multimedia Computing and Service, 2014, pp. 319–322.*

[16] S. Li, J. Shang, Z. Duan, and J. Huang, "Fast detection method of quick response code based on run-length coding," *IET Image Processing, vol. 12, no. 4, pp. 546–551, 2018.*

[17] L. Blanger and N. S. T. Hirata, "An evaluation of deep learning techniques for QR code detection," *Proceedings of the IEEE International Conference on Image Processing (ICIP), Taipei, Taiwan, pp.1625–1629, 2019.*

[18] L. Karrach, E. Pivarciova, and P. Bozek, "Recognition of perspective distorted QR codes with a partially damaged finder pattern in real scene images," *Applied Sciences, Vol. 10, no. 21, p. 7814, 2020.*

[19] T. H. Chou, C. S. Ho, and Y. F. Kuo, "QR code detection using convolutional neural networks," *Proceedings of 2015 International Conference on Advanced Robotics and Intelligent Systems (ARIS)," Taipei, Taiwan,2015, pp. 1–5.*

[20] W. C. Kurniawan, H. Okumura, Muladi, and A. N. Handayani, "An improvement on QR code limit angle detection using convolution neural network," *Proceedings of 2019 International Conference on Electrical, Electronics and Information Engineering (ICEEIE), Denpansar, Indonesia, 2019, pp.234–238.*

[21] L. Yang and Q. Feng, "The improvement of Bernsen binarization algorithm for QR Code image," *Proceedings of 5th IEEE International Conference on Cloud Computing and Intelligent Systems (CCIS), Nanjing, China, 2018, pp.931–934.*

[22] R. M. Haralick, "Statistical and structural approaches to texture," *Proceedings of the IEEE, vol. 67, no. 5, 1979, pp. 786–80.*

[23] X. Huang, X. Liua, and L.Zhang , "A multichannel gray level co-occurrence matrix for multi-hyperspectral image texture representation," *Remote Sensing, vol. 6, no. 9, pp. 8824–8445, 2014.*

[24] P. K. Mall, P. K. Singh, and D. Yadav, "GLCM based feature extraction and medical X-RAY image classification using machine learning techniques," *Proceedings of IEEE Conference on Information and Communication Technology, Allahabad, India, 2019, pp. 1–6.*

[25] R. Tekin, O. F. Ertugrul, and Y. Kaya, "New local binary pattern approaches based on color channels in texture classification," *Multimedia Tools and Applications, vol. 79, no. 43, pp. 32541–32561, 2020.*

[26] S H. Khaleefah, S. A. Mostafa, A. Mustafa, and M. F. Nasrudin, "Review of localbinary pattern operators in image feature extraction," *Indonesian Journal of Electrical Engineering and Computer Science, vol. 19, no. 1, pp. 23–31, 2020.*

[27] QR code dataset : QR Codes | Kaggle